Structure–function analysis of manganese exporter proteins across bacteria

Received for publication, April 10, 2017, and in revised form, January 26, 2018 Published, Papers in Press, February 13, 2018, DOI 10.1074/jbc.M117.790717

Rilee Zeinert[‡1], Eli Martinez[‡2], Jennifer Schmitz[‡2], Katherine Senn[‡2], Bakhtawar Usman[‡], Vivek Anantharaman[§], L. Aravind[§3], and Lauren S. Waters[‡4]

From the [‡]Department of Chemistry, University of Wisconsin, Oshkosh, Wisconsin 54901 and the [§]National Center for Biotechnology Information, National Library of Medicine, National Institutes of Health, Bethesda, Maryland 20894

Edited by Chris Whitfield

Manganese (Mn) is an essential trace nutrient for organisms because of its role in cofactoring enzymes and providing protection against reactive oxygen species (ROS). Many bacteria require manganese to form pathogenic or symbiotic interactions with eukaryotic host cells. However, excess manganese is toxic, requiring cells to have manganese export mechanisms. Bacteria are currently known to possess two widely distributed classes of manganese export proteins, MntP and MntE, but other types of transporters likely exist. Moreover, the structure and function of MntP is not well understood. Here, we characterized the role of three structurally related proteins known or predicted to be involved in manganese transport in bacteria from the MntP, UPF0016, and TerC families. These studies used computational analysis to analyze phylogeny and structure, physiological assays to test sensitivity to high levels of manganese and ROS, and inductively coupled plasma–mass spectrometry (ICP-MS) to measure metal levels. We found that MntP alters cellular resistance to ROS. Moreover, we used extensive computational analyses and phenotypic assays to identify amino acids required for MntP activity. These negatively charged residues likely serve to directly bind manganese and transport it from the cytoplasm through the membrane. We further characterized two other potential manganese transporters associated with a Mn-sensing riboswitch and found that the UPF0016 family of proteins has manganese export activity. We provide here the first phenotypic and biochemical evidence for the role of Alx, a member of the TerC family, in manganese homeostasis. It does not appear to export manganese, but rather it intriguingly facilitates an increase in intracellular manganese concentration. These findings expand the available knowledge about the identity and mechanisms of manganese homeostasis proteins across bacteria and show that proximity to a Mn-responsive riboswitch can be used to identify new components of the manganese homeostasis machinery.

Transition metals are essential for life, as they play important roles as enzyme cofactors and structural components of proteins and RNAs. Reflecting this fact, one-third of the proteomes of organisms from bacteria to humans consist of metalloproteins (1, 2). In bacteria, metal availability is intimately involved in pathogenesis. Bacteria unable to maintain proper metal homeostasis are less virulent, and mammalian hosts actively seek to withhold essential metals from invading bacteria (3, 4). Yet in excess, metals are toxic to cells. This toxicity typically results from metal-dependent oxidative damage (*e.g.* the Fenton reaction) and/or the displacement of cognate metals from their binding sites by the metal that is in excess (3, 5–8). Thus, cells have a battery of metal importers, exporters, sequestration factors, and regulators to carefully control the intracellular level of each metal (1, 2, 9, 10).

Of the transition metals, manganese is particularly important for cells experiencing oxidative stress. Manganese aids in detoxifying reactive oxygen species (ROS)[5] through at least three independent mechanisms: by serving as a cofactor for enzymes like Mn-SOD that break down ROS, by forming low-molecular-weight complexes with small molecules that non-enzymatically degrade ROS, and by transiently replacing iron in the active sites of certain enzymes to avoid oxidative damage to the proteins (3, 11, 12). It also serves as an enzyme cofactor for diverse enzymes important for cell metabolism (13, 14). These roles make manganese of prime importance in situations where bacteria encounter high levels of ROS, such as during interactions with eukaryotic host cells during pathogenesis and symbiosis.

However, high levels of manganese are toxic. Overaccumulation of manganese is often correlated with deficiencies in other metal pools. This can then cause mismetallation of regulatory transcription factors and key enzymes, affecting growth,

This work was supported by the Intramural Research Program of the National Library of Medicine, National Institutes of Health (to V. A. and L. A.), Grants 22658 and 23595 from the Research Corporation for Scientific Advancement (to L. S. W.), the Department of Education TRIO McNair Scholars Program at the University of Wisconsin, Oshkosh (to R. Z. and E. M.), and University of Wisconsin, Oshkosh, Faculty Development funds (to L. S. W.). The authors declare that they have no conflicts of interest with the contents of this article. The content is solely the responsibility of the authors and does not necessarily represent the official views of the National Institutes of Health.

This article contains supporting "Experimental procedures," Figs. S1–S6, and Tables S1–S3.

[1] Present address: Molecular and Cellular Biology Graduate Program, University of Massachusetts, Amherst, MA 01003.

[2] These authors contributed equally to this work.

[3] To whom correspondence may be addressed. Tel.: 301-594-2445; Fax: 301-435-7794; E-mail: aravind@ncbi.nlm.nih.gov.

[4] To whom correspondence may be addressed. Tel.: 920-424-7099; Fax: 920-424-2042; E-mail: watersl@uwosh.edu.

[5] The abbreviations used are: ROS, reactive oxygen species; CDF, cation diffuser facilitator; Fur, ferric uptake regulator; TM, transmembrane; ILT, iron–lead transporter; ICP-MS, inductively coupled plasma–mass spectrometry; Bistris propane, 1,3-bis[tris(hydroxymethyl)methylamino]propane (BTP); SPA, sequential peptide affinity.

sensitivity to ROS, and virulence (3, 6, 15–18). For example, in *Escherichia coli*, excess intracellular manganese results in aberrantly low levels of iron through the action of Mn-Fur (ferric uptake regulator), which shuts down iron uptake. Heme-containing enzymes are no longer active, and cells cease to grow (15). Therefore, cells need to have mechanisms, including manganese exporters, to withstand high environmental manganese and to control protein metallation in the cytoplasm.

Cells possess robust manganese homeostasis systems that control intracellular manganese levels to prevent toxicity while maintaining sufficient manganese levels. Two main types of manganese exporters have been identified in bacteria: MntE, a cation diffuser facilitator (CDF) family protein; and MntP, with a 6-transmembrane helix topology typical of the so-called LysE superfamily of transporters (19–24). Both classes of exporters are broadly conserved and represented across bacteria. A third class of potential manganese exporter is represented by the CtpC protein of *Mycobacterium tuberculosis*, a P-type ATPase that transports manganese and/or zinc (25, 26). Additionally, there are two main types of manganese importers: MntH, which uses the proton motive force to power uptake of manganese; and an ABC cassette importer known in Gammaproteobacteria as SitABCD (3, 9, 10, 14). The expression of these genes is typically regulated by the MntR transcription factor, which upon binding of manganese undergoes a conformational change that allows it to bind DNA (10, 14, 18). Laboratory strains of *E. coli* possess the MntH importer, the MntP exporter, and two other genes regulated by MntR: *dps*, which encodes the metal-binding ferritin family protein and *mntS*, which encodes a small protein (27).

Manganese exporters are critical for proper manganese homeostasis and cell function. In the absence of either of the manganese exporters *mntE* or *mntP*, bacteria are highly sensitive to manganese stress, accumulate excess intracellular manganese, and are less pathogenic (19–22, 28). The CtpC manganese/zinc exporter also contributes to *M. tuberculosis* virulence (25, 26). The MntE exporter protein has been well-characterized: its structure has been modeled, and the amino acids contributing to its function and metal specificity have been determined (5, 19, 28–30). In contrast, little is known about the MntP exporter protein. Its structure, the amino acids involved in transporting manganese, and the mechanism of metal specificity remain unknown.

Although the MntP protein remains relatively uncharacterized, the regulation of *mntP* gene expression has been deciphered. In *E. coli*, the *mntP* gene has been shown to be transcriptionally and post-transcriptionally regulated by manganese levels through the transcription MntR factor and the *yybP-ykoY* riboswitch (20, 31). The *yybP-ykoY* riboswitch directly and specifically binds manganese and regulates gene expression by ribosome-binding site sequestration or termination/antitermination mechanism in different organisms (31, 32). Intriguingly, the *yybP-ykoY* riboswitch is very broadly conserved across bacteria, suggesting an important role for manganese homeostasis. Bioinformatic analysis of the genes associated with the *yybP-ykoY* riboswitch revealed 27 protein families, most of which remain biochemically uncharacterized (31). Of these, 10 protein families are predicted to be membrane proteins with conserved charged residues in the transmembrane regions, indicative of ion transport. We predicted that one or more of these proteins may be novel manganese exporters (31). In a more recent survey of 2774 prokaryotic genomes, with representatives from across major prokaryotic lineages characterized to date, we found that only 28.7% have a predicted *mntP* gene, suggesting that there might be alternative manganese transporters.

In this study, we set out to characterize the structure and function of the MntP protein as well as identify new manganese exporters across bacteria. Using several different growth assays, we identified essential amino acids for MntP activity, including highly conserved Asp and Glu residues that likely create the negatively charged binding surface for the manganese cation. We also showed that unregulated MntP activity contributes to oxidative stress. Additionally, we investigated the best candidates for novel manganese exporters among the uncharacterized genes genomically linked to the *yybP-ykoY* riboswitch. Consequently, we found that MneA, a member of the UPF0016 family, is a new type of manganese exporter. In contrast, under similar test conditions, we were unable to obtain evidence that Alx, a member of the TerC family, is directly involved in manganese efflux. Rather, Alx leads to manganese import.

Results

MntP provides robust manganese resistance and affects resistance to ROS

MntP is required for growth of *E. coli* and other bacteria in high manganese conditions (20–22). We have shown previously that Δ*mntP* cells lacking the MntP exporter cannot grow in the presence of 1 mM $MnCl_2$ on plates or 0.5 mM $MnCl_2$ in liquid culture (15, 20). To further define the amount of manganese tolerated by the wild type and the Δ*mntP* strain, we tested a range of manganese concentrations using several quantitative assays. These assays showed that the Δ*mntP* strain can only tolerate up to ~0.1 mM supplemental $MnCl_2$, whereas a strain producing MntP can grow in the presence of up to ~5 mM $MnCl_2$ (Fig. 1, *A–C*). Wildtype *E. coli* cells typically contain ~5–15 μM manganese, whereas Δ*mntP* cells accumulate ~50 μM manganese (15, 20, 33, 34). This suggests that in a wildtype strain background, MntP confers a resistance to a 50-fold excess of supplemental manganese (5 mM supplemental $MnCl_2$ to 0.1 mM supplemental $MnCl_2$) and can reduce intracellular manganese levels by 500-fold (5 mM extracellular concentration to 10 μM intracellular concentration).

We also sought to identify other growth-based phenotypes for *mntP*. As manganese is intimately linked to the ability to withstand ROS, we wondered whether MntP modulates the ability to survive ROS stress. We examined this by testing whether MntP expression affected the growth of a strain that accumulates high levels of hydrogen peroxide.

The well-characterized Hpx⁻ strain (Δ*ahpCF* Δ*katG* Δ*katE*) lacks three enzymes that scavenge hydrogen peroxide and accumulate millimolar levels of hydrogen peroxide (35). High levels of manganese are required by Hpx⁻ cells to withstand the elevated levels of hydrogen peroxide. Indeed, Hpx⁻ cells without the MntH manganese importer cannot grow aerobically

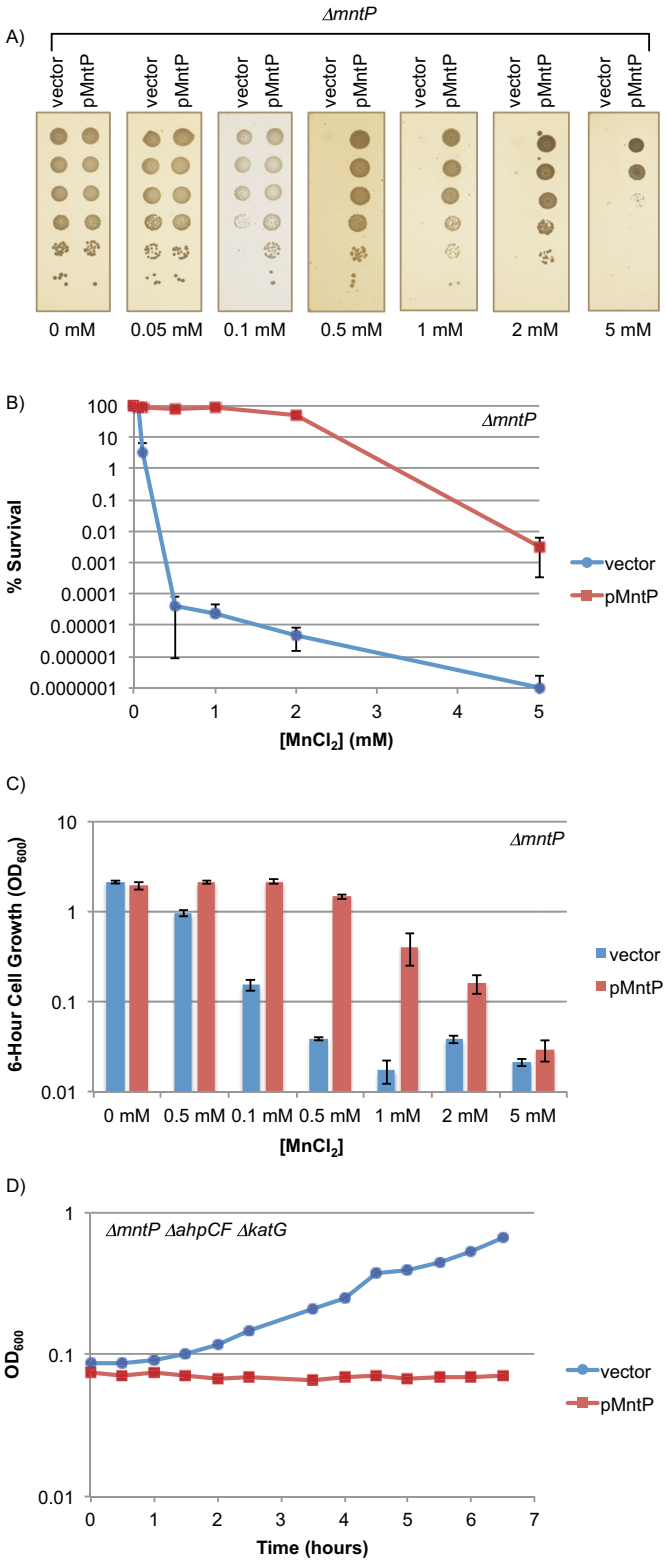

Figure 1. Manganese and H_2O_2 sensitivity is associated with a lack or excess of MntP. *A*, cells lacking *mntP* show pronounced sensitivity to manganese at external levels above 0.1 mM in LB medium. 10-fold serial dilutions of mid-exponential–phase cultures of Δ*mntP* cells (MS047) bearing the pBAD24 empty vector or pBAD24-MntP (pLW132) were spotted onto LB plates containing 0.2% arabinose, 150 μg/ml ampicillin, and the indicated amounts of $MnCl_2$. *B*, dilutions of mid-exponential–phase cultures of the strains from *A* were spread onto LB plates containing 0.2% arabinose, 150 μg/ml ampicillin, and the indicated amounts of $MnCl_2$, and viable colony-forming units were counted for each dose of $MnCl_2$. *C*, mid-exponential–phase cultures of the strains from *A* were diluted into LB medium containing 0.2% arabinose, 150 μg/ml ampicillin, and the indicated amounts of $MnCl_2$, and cell growth was monitored after 6 h. *D*, cells ectopically producing MntP under conditions of oxidative stress show a pronounced growth defect. Exponential-phase cultures of Δ*mntP* Δ*ahpCF* Δ*katG* cells (RDZ5) bearing the pBAD24 empty vector or pBAD24-MntP (pLW132) were grown in M9 minimal medium with 0.2% arabinose and 150 μg/ml ampicillin. For *B* and *C*, the *error bars* indicate the standard deviations from three replicates of one experiment. For all panels, the data are representative of at least three independent experiments.

(33). To avoid anaerobic pre-growth of cultures before growth assays, we used a strain lacking two of the hydrogen peroxide–degrading enzymes (Δ*ahpCF* Δ*katG*) and pre-grew strains in the presence of pyruvate (a ROS scavenger) and $MnCl_2$ (to aid in ROS detoxification). In this sensitized strain background, we reasoned that excess MntP would lead to the efflux of manganese and consequently an inability to grow.

We deleted the *mntP* gene in this sensitized strain background (Δ*ahpCF* Δ*katG*) and monitored the ability of MntP to cause a cessation of growth. Cells were grown into log phase initially in M9 minimal medium with glucose and supplemental pyruvate and $MnCl_2$ to promote growth. Cells were then collected by centrifugation, washed, and resuspended in M9 medium without pyruvate and $MnCl_2$ to allow intracellular ROS to accumulate. Arabinose was included to induce protein production. We observed that the sensitized Δ*mntP* strain with the empty vector was able to grow. However, the cells producing MntP protein stopped growing upon induction of MntP expression in the presence of high concentrations of ROS (Fig. 1*D*). This observation demonstrates that MntP production affects resistance to reactive oxygen species.

Identification of conserved residues required for activity of the MntP family

The regulation of the *mntP* gene is well understood, but less is known about the structure and function of the MntP protein. Accordingly, we carried out a computational analysis of the MntP protein using a combination of sequence–profile searches, profile–profile comparisons, and transmembrane (TM) topology prediction. The MntP protein possesses six TM helices with characteristic conserved charged amino acids (Fig. 2*A*). Profile–profile comparisons confirmed that MntP belonged to the LysE superfamily of transporters. Further, they showed that the six-helical members of this family have emerged from the tandem duplication of a core ancestral unit with three membrane-spanning α-helices. Importantly, they also revealed that within this superfamily, MntP formed a higher-order clade with the following distinct families: 1) MntP; 2) a cadmium resistance transporter (Cad); 3) the UPF0016 family; 4) the TerC family; and 5) the iron–lead transporter (ILT) family (Fig. 2*B*). All of these families are unified by the presence of a highly conserved acidic residue (Asp or Glu) inside the first TM helix of each of the core trihelical units (Fig. 2*A*), which is absent in all other families of the LysE superfamily, including LysE itself. The characterized members of this higher-order clade (MntP, Cad, TerC, and ILT) are all implicated in transporting heavy metals/metalloids across membranes, suggesting that a common mechanism is used across this clade in this process.

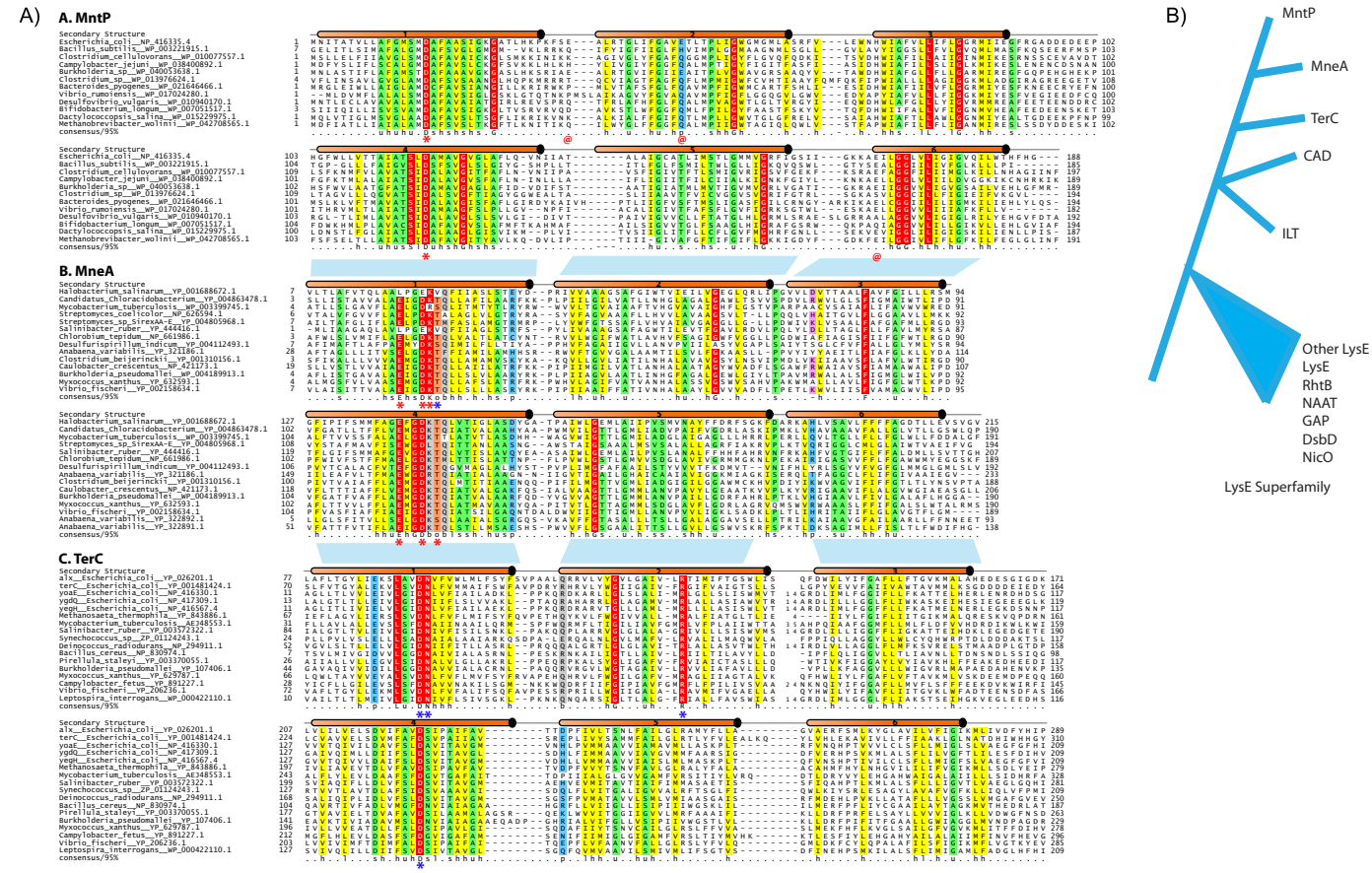

Figure 2. Multiple sequence alignments of MntP, MneA, and TerC reveal key amino acids for function. *A*, representative multiple sequence alignments of the MntP, MneA, and TerC families are shown with a 95% consensus. The *numbered* transmembrane regions are shown above the alignment as *orange cylinders*. The sequences are denoted by their gene names or locus tags, species names, and accessions. The *numbers* within the alignment represent poorly conserved inserts of the given number of amino acid residues that are not shown. Within each family, the two trihelical units are aligned with each other. The equivalence of the three transmembrane regions among the three families is also illustrated with *blue rectangles*. Residues that were shown to be critical for MntP or MneA activity by mutagenesis are shown with a *red star*, and those with intermediate effects are shown with a *red* @ symbol. Other residues predicted to contribute significantly to protein activity are shown with a *blue star*. The coloring is based on the consensus of the whole family alignment: "h" is for hydrophobic residues (ACFILMVWY (*yellow*)); "l" represents the aliphatic subset of the hydrophobic class (ILV (*yellow*)); "s" represents small residues (ACDGNPSTV (*green*)); "u" represents the tiny subclass of small residues (GAS (*green*)); "p" represents polar residues (CDEHKNQRST (*blue*)); "c" represents the charged subclass of polar residues (DEHKR (*pink*)); "—" represents the negative subclass of charged residues (DE); "o" represents alcoholic residues (ST (*orange*)); and "b" represents big residues (KFILMQRWYE (*gray*)). Any absolutely conserved residue is labeled and *shaded red*. *B*, phylogenetic profile of the higher-order clade within the LysE superfamily that includes MntP, UPF0016, TerC, CAD, and ILT.

A comprehensive multiple sequence alignment of 3078 MntP orthologs from diverse bacterial lineages predicted high functional importance for the two acidic residues from the first helix of each of the trihelical units (Asp-16 and Asp-118 in *E. coli*). We inferred that these characteristic acidic residues from each of the two trihelical units that constitute the six-helix TM module of MntP are likely to support an intramembrane negatively charged pore that directs the efflux of the manganese cation. Additionally, it also allowed us to identify a few less-conserved acidic residues within or in the vicinity of the TM helices (Glu-35, Glu-47, and Glu-167 with 80, 95, and 90% conservation of polar residues, respectively) as having potential, although relatively less important, roles.

Charged transmembrane residues are essential for MntP activity in the manganese sensitivity assay

To test the predictions that Asp-16, Asp-118, Glu-35, Glu-47, and Glu-167 might interact with manganese in MntP, we mutated these acidic residues and other conserved amino acids and assayed the ability of the mutant MntP proteins to rescue Δ*mntP* phenotypes. We made a panel of MntP mutants expressed from an inducible promoter on a plasmid and examined whether the MntP mutants could restore normal growth to a Δ*mntP* strain grown with $MnCl_2$ (Fig. 3).

Of the 14 mutants tested, five mutants were unable to fully rescue the Δ*mntP* manganese growth defect. Consistent with our predictions, two mutants, D16A and D118A, were unable to grow at all on plates with 1 mM $MnCl_2$ (Fig. 3*A*). These mutations completely abolished MntP functionality. Three mutants, E35A, E47A, and E167A, had intermediate phenotypes. The E47A mutant displayed a significant growth defect on plates with 1 mM $MnCl_2$, whereas the E167A and E35A mutants complemented the Δ*mntP* defect on plates with 1 mM $MnCl_2$ but only partially restored growth on plates with 5 mM $MnCl_2$. These phenotypes were also observed in liquid culture, where the D16A and D118A mutants could not rescue the Δ*mntP* growth defect at all (Fig. 3*B*). As on the plates, the E47A mutant also displayed a severe growth defect, whereas the E167A

mutant had a moderate loss of growth and the E35A mutant had a mild growth defect discernable only at high-manganese concentrations (Fig. 3*B*). Like the Asp-16 and Asp-118 residues, Glu-47 is located within TM helix-2 for the first trihelical unit. In contrast, Glu-167 is predicted to be close to the cytoplasmic end of TM helix-6, and Glu-35 is located in a predicted cytoplasmic loop between TM domains 1 and 2 (Fig. 2*A*).

To confirm that the inability of these five mutants to restore growth on manganese to the Δ*mntP* strain was due to a defective MntP protein rather than a lack of expression, we created partially functional epitope-tagged versions that acted similarly in restoring growth on manganese to the Δ*mntP* strain (Fig. 4*A*) and examined the levels of the tagged versions of the five mutants that displayed a phenotype (Fig. 4*B*). We observed that all of these mutant MntP proteins were present at levels similar to the wildtype MntP expressed from the plasmid. Thus, each of these amino acids is required for full activity of the protein.

We also tested the effects of mutating eight other less conserved amino acids that could potentially coordinate manganese, including two His residues and a negatively charged patch of six Asp or Glu residues in the linker region between the two trihelical units. Each of these single mutants, as well as a triple mutant, showed no reduction in MntP activity, even on plates with 5 mM $MnCl_2$ (Fig. 3*A*). These data indicate that only the strongly conserved acidic residues but not the less conserved His and negatively charged linker play a substantial role in manganese cation export.

Charged transmembrane residues are essential for MntP activity in the ROS sensitivity assay

We next tested whether these *mntP* alleles could confer a cessation of growth in the ROS-sensitized strain background (Δ*ahpCF* Δ*katG*) (Fig. 5). Because manganese is required in this strain to survive the high intracellular H_2O_2 levels, production of the wildtype MntP caused a lack of growth (Fig. 1*D*). Any *mntP* mutants that failed to halt growth would therefore be defective in MntP activity.

We observed similar phenotypes for the mutants in this reactive oxygen species sensitivity assay (Fig. 5) as for the manganese sensitivity assay (Fig. 3). Cells producing the D16A and D118A MntP mutants were able to grow similarly to the cells with the empty vector, indicating a lack of manganese export. Strains bearing the E35A, E47A, and E167A mutant versions of MntP displayed an intermediate phenotype between strains with the empty vector or wildtype MntP. This suggests that these MntP proteins are only partially functional and, therefore, that these acidic amino acids contribute to activity. We noted that this phenotype was somewhat variable, possibly as a result of the significant oxidative stress that the cells experienced during pre-growth. Lastly, cells with the H29A or H70A mutation or with mutations in the negatively charged patch showed a lack of growth similar to cells with wildtype MntP, indicating robust manganese export and normal MntP activity.

Taken together, these results show that the Asp-16 and Asp-118 residues are strictly required for MntP manganese export, whereas the Glu-35, Glu-47, and Glu-167 residues contribute to MntP activity, and the His-29, His-70, and Asp-94–Glu-98 residues are dispensable for MntP function.

The UPF0016 family proteins are predicted to be novel manganese exporters

Having characterized the MntP protein from *E. coli*, we next wondered if we could use these approaches to identify additional unknown manganese export proteins in *E. coli* or other bacteria. Because the *mntP* gene is regulated by a manganese-sensing riboswitch element called *yybP-ykoY* (31, 32), we investigated whether any other genes preceded by this riboswitch could encode novel manganese exporters.

Of the 1294 bacterial strains analyzed that possessed the riboswitch, the *yybP-ykoY* riboswitch was frequently associated with four main protein families: TerC/Alx/YkoY (731 out of 763 strains), P-type ATPase (308 out of 312 strains), UPF0016, (328 out of 333 strains), and MntP (293 strains). These four families all possessed transmembrane regions with conserved charged amino acids, suggesting that these could be manganese exporters. Of these families, a previous study had suggested that the P-type ATPase might have a role in the export of manganese in firmicutes (32). Both UPF0016 and TerC belong to the same higher-order clade of the LysE superfamily as MntP and share the conserved acidic residue in each of the core three-helix TM units (Fig. 2). Hence, we decided to further investigate these as candidate manganese transporters. Notably, UPF0016 showed a mutually exclusive phyletic pattern with respect to MntP, indicating that it performs the same role as MntP (Fig. 9*B*). This apparent functional equivalence predicted by comparative genomics made it the best candidate as an alternative manganese exporter.

UPF0016 family proteins occur either as just a single copy of the trihelical ancestral unit of the LysE superfamily or as duplicate copies of this unit in the same polypeptide. To identify potentially important functional residues, we prepared a comprehensive multiple sequence alignment of 424 UP0016 orthologs from phylogenetically diverse bacteria. This allowed us to identify, in addition to the highly conserved acidic residue in the first helix of the trihelical TM unit, two other conserved strongly charged/polar residues in each of the trihelical TM units (Fig. 2*A*). The common evolutionary origin of MntP and UPF0016, along with similar conserved acidic residues in the first helix of the trihelical ancestral unit, suggested that UPF0016 like MntP might form a comparable transmembrane pore lined with acidic residues that direct the efflux of manganese cations.

Complementation and mutational analysis establishes UPF0016 family protein as a new manganese exporter MneA

We next tested whether UPF0016 proteins preceded by the *yybP-ykoY* riboswitch could export manganese out of cells. We cloned the genes for the UPF0016 protein from *Streptomyces* sp. SirexAA-E and *Vibrio fischeri* into a plasmid vector and examined whether they could rescue the observed manganese sensitivity and the ROS sensitivity growth defects of the *E. coli* Δ*mntP* strain (Fig. 1).

Upon exposure to manganese, we observed that the UPF0016 protein could indeed complement the Δ*mntP* manganese sensitivity on plates and in liquid (Fig. 6, *A* and *B*). This suggests that the UPF0016 protein represents a new class of manganese

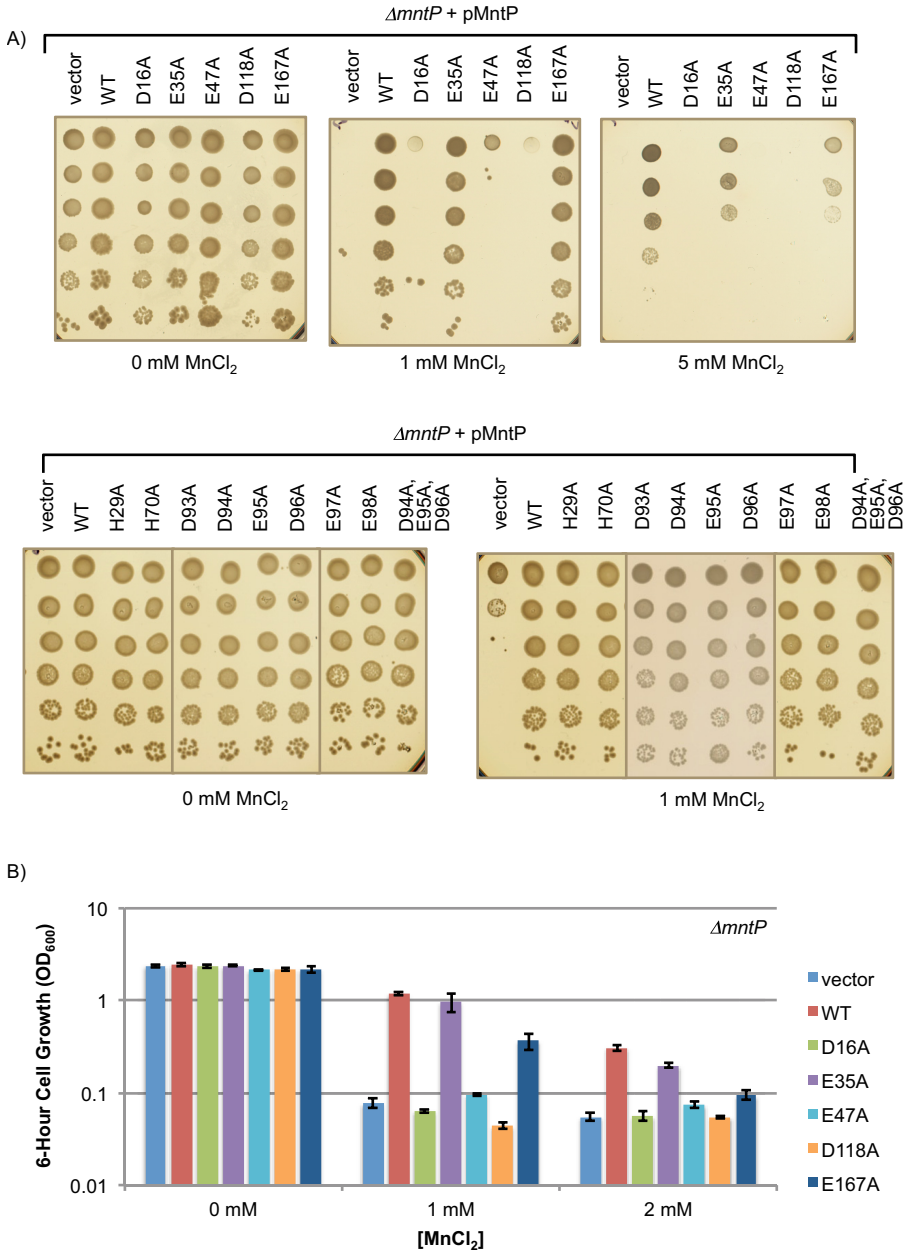

Figure 3. Mutations in conserved, charged amino acids impair MntP activity and lead to manganese sensitivity. *A*, 10-fold serial dilutions of mid-exponential–phase cultures of Δ*mntP* cells (MS047) bearing the pBAD24 empty vector, pBAD24-MntP (pLW132), or pBAD24-MntP with the specified amino acid mutations were spotted onto LB plates containing 0.2% arabinose, 150 μg/ml ampicillin, and the indicated amounts of $MnCl_2$. The mutant pBAD24-MntP plasmids used were: pRZ1 (D16A), pRZ11 (H29A), pRZ2 (E35A), pPM1 (E47A), pPM3, (H70A), pRM2 (D93A), pRZ10 (D94A), pPM8 (E95A), pRZ12 (D96A), pPM9 (E97A), pPM10 (E98A), pRZ3 (D118A), pPM2 (E167A), and pRM3 (E94A,E95A,D96A). *B*, mid-exponential–phase cultures of the strains from *A* were diluted back into LB medium containing 0.2% arabinose, 150 μg/ml ampicillin, and the indicated amounts of $MnCl_2$, and cell growth was monitored after 6 h. For *B*, the *error bars* indicate the standard deviations from three replicates of one experiment. For all panels, the data are representative of at least three independent experiments.

exporter. Indeed, while this work was in progress, the UPF0016 protein from *V. cholerae* was independently shown to export manganese and named MneA (36). The *mneA* gene from *Streptomyces* could only rescue growth on plates up to 0.5 mM $MnCl_2$, whereas the *mneA* gene from *Vibrio* could only fully restore growth up to 1 mM $MnCl_2$, compared with the native *mntP* gene from *E. coli*, which allowed growth up to and beyond 2 mM $MnCl_2$ (Fig. 6*A*). The reduced ability of the *Streptomyces* protein to complement the Δ*mntP* manganese sensitivity is likely due to the greater evolutionary distance of *Streptomyces* from *E. coli* relative to *Vibrio* and *E. coli*.

We then examined whether MneA similar to MntP, also affected the sensitivity to reactive oxygen species. If expression of MneA caused a growth defect in the ROS-sensitized strain background, it would be additional evidence that MneA expression leads to a decrease in manganese levels. Indeed, we observed that expression of MneA in the Δ*ahpCF* Δ*katG* strain background caused a block in growth (Fig. 6*C*) consistent with an ability to efflux manganese out of cells. Even supplemental manganese provided in the media could not rescue the growth defect (Fig. S1), further supporting a role for MneA as a robust manganese exporter.

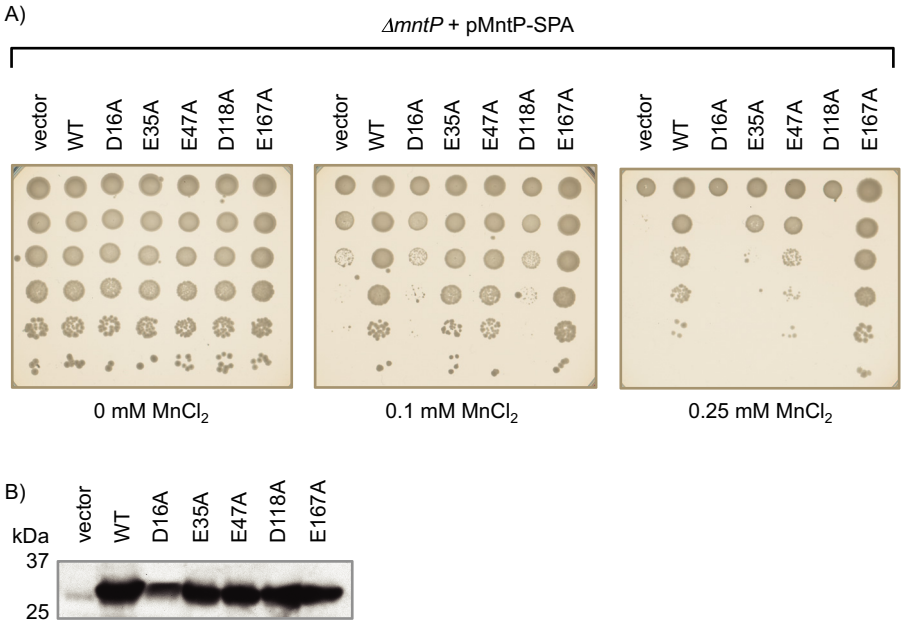

Figure 4. Defective MntP mutants are expressed similarly to wildtype MntP. *A*, epitope-tagged MntP mutants display similar manganese resistance as the untagged constructs. 10-fold serial dilutions of mid-exponential–phase cultures of Δ*mntP* cells (MS047) bearing the pBAD24 empty vector, pBAD24-MntP-SPA (pRZ19), or pBAD24-MntP-SPA with the specified amino acid mutations were spotted onto LB plates containing 0.2% arabinose, 150 μg/ml ampicillin, and the indicated amounts of $MnCl_2$. The mutant pBAD24-MntP-SPA plasmids used were: pRZ20 (D16A), pRZ24 (E35A), pRZ21 (E47A), pRZ22 (D118A), and pRZ23 (E167A). *B*, Western blot analysis of MntP-SPA levels produced from Δ*mntP* cells (MS047) shown in *A* bearing the pBAD24 empty vector, pBAD24-MntP-SPA (pRZ19), or pBAD24-MntP-SPA with the amino acid mutations specified in *A*. For all panels, the data are representative of at least three independent experiments.

To validate that MneA was being produced in the heterologous *E. coli* system, we generated a partially functional epitope-tagged version of MneA that restored growth on manganese to the Δ*mntP* strain and observed that the MneA protein was present (Fig. 6, *D* and *E*).

To test whether MneA could change the intracellular manganese levels, we carried out ICP-MS analysis from cells grown in Luria broth (LB) medium containing 0.5 mM $MnCl_2$ (Table 1). The Δ*mntP* strain with the empty vector had an intracellular manganese concentration of 92 μM, similar to previously observed levels (~50–100 μM) (15, 20). The Δ*mntP* strain expressing MneA had 2.8-fold lower intracellular manganese (34 μM), similar to the levels measured for WT strains with intact native *mntP* (~15–25 μM) (15, 20, 33). These observations are consistent with robust manganese export by MneA.

Using ICP-MS analysis and growth assays, we also tested whether MneA contributed to the export of other metals. We measured the intracellular levels of zinc, copper, and nickel in cells grown in LB medium. Zinc levels were 1.5-fold lower, copper levels were 1.3-fold lower, and nickel levels were 1.2-fold lower in cells expressing MneA relative to cells with the empty vector (Table 2). Moreover, when grown on LB plates containing various metals, Δ*mntP* cells producing MneA did not show any increased resistance to calcium, cobalt, copper (II), iron (II) and (III), magnesium, nickel, or zinc at concentrations where control cells bearing the empty plasmid showed markedly slower growth (data not shown). These results are consistent with the activity of MneA being specific for manganese export.

We next examined the role of the highly conserved charged and polar amino acids in the predicted transmembrane domains of MneA. As was done for MntP, the residues were mutated to Ala, and the ability of the mutant *Vibrio* MneA proteins to rescue the manganese sensitivity of the Δ*mntP* strain was tested. These included: E19A, D22A, and K23A, which lie inside the first helix of the first trihelical unit, and E116A, D119A, and T121A, which lie in the first helix of the second trihelical unit. We observed that none of the mutants was able to restore growth to the Δ*mntP* strain on manganese plates (Fig. 7*A*). Thus, all of the mutations completely abolished MneA activity in the manganese sensitivity assay, consistent with their strong conservation. To confirm expression of the mutant proteins, we created epitope-tagged versions of the mutants that acted equivalently to the untagged mutants and were unable to rescue the Δ*mntP* growth defect (Fig. 7*B*). All of the tagged mutant MneA proteins were present at levels similar to the wildtype MneA expressed from the plasmid (Fig. 7*C*), indicating the importance of each amino acid for manganese export. These observations supported the hypothesis based on our sequence analysis and structure prediction that these residues line an intramembrane charged conduit for the passage of the manganese cation.

The TerC family protein Alx does not directly export manganese in LB medium

The TerC family of proteins is the group of open reading frames most frequently associated with the Mn-binding *yybP-ykoY* riboswitch and shares a specific common ancestry and conserved residues with MntP and MneA (Fig. 2*B*). In *E. coli*, two paralogous copies of the *yybP-ykoY* riboswitch are present upstream of the genes *mntP* and *alx*, which encodes a TerC family protein. These riboswitches confer manganese induction to both genes (31). However, unlike MneA and MntP,

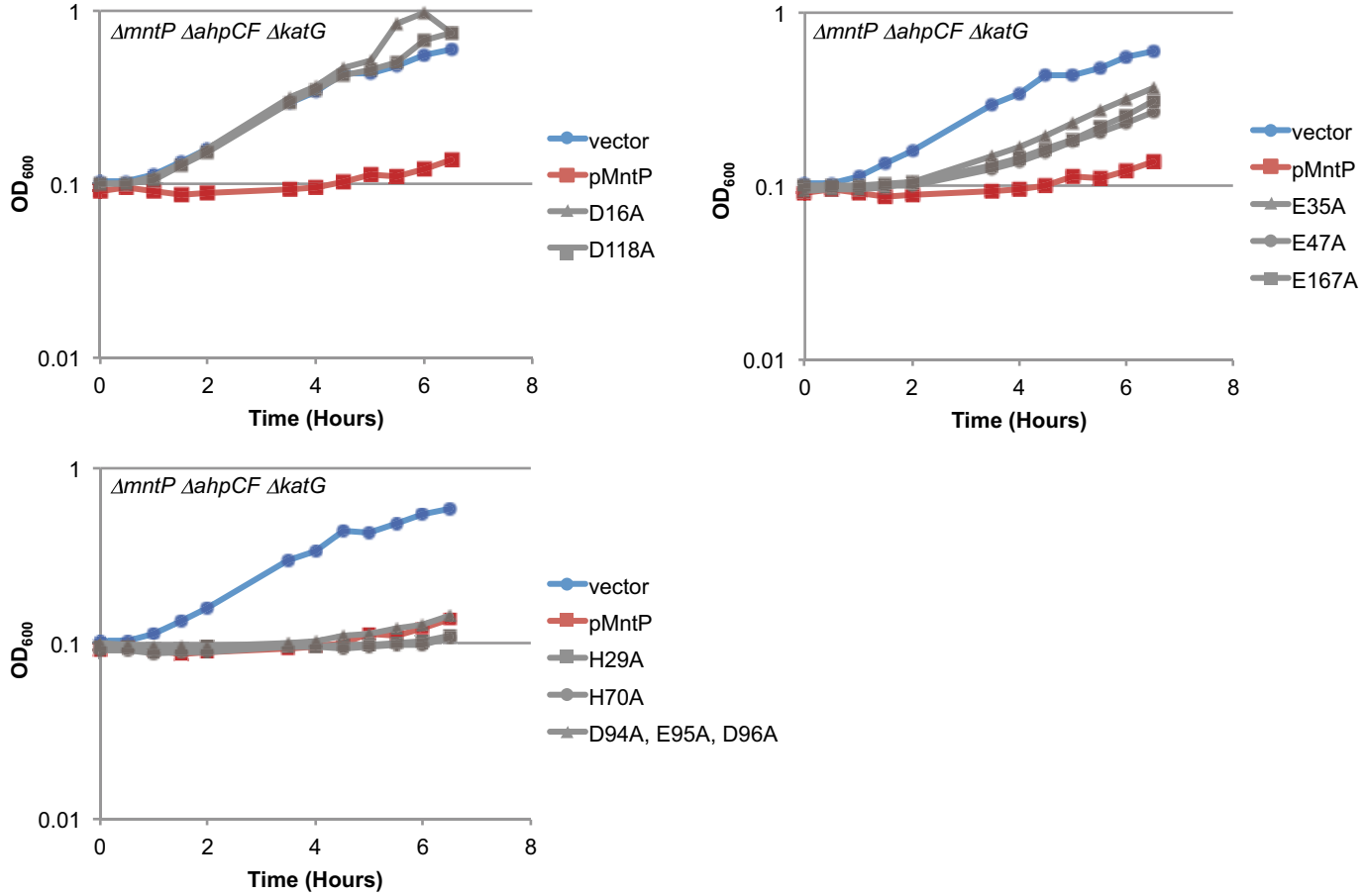

Figure 5. Mutations in conserved, charged amino acids impair MntP activity and prevent H_2O_2 sensitivity upon ectopic expression. Exponential-phase cultures of Δ*mntP* Δ*ahpCF* Δ*katG* cells (RDZ5) bearing the pBAD24 empty vector, pBAD24-MntP (pLW132), or pBAD24-MntP with the specified amino acid mutations were grown in M9 minimal medium with 0.2% arabinose and 150 μg/ml ampicillin. The mutant pBAD24-MntP plasmids used were: pRZ1 (D16A), pRZ11 (H29A), pRZ2 (E35A), pPM1 (E47A), pPM3, (H70A), pRZ3 (D118A), pPM2 (E167A), and pRM3 (E94A,E95A,D96A). Data are representative of at least three independent experiments.

which show a strong mutually exclusive phyletic pattern, Alx tends to co-occur with either MneA or MntP, indicating that it has a distinct role compared with those exporters.

To investigate the ability of Alx to affect manganese export, we also expressed Alx in the previously described Δ*mntP* mutant strains. In the manganese sensitivity assay, we observed that the Alx protein could not restore growth on LB medium with high $MnCl_2$ to the Δ*mntP* strain (Fig. 8, *A* and *B*). To confirm that Alx was being produced, we examined the expression of an epitope-tagged version of Alx and observed that the Alx protein was indeed being expressed (Fig. 8, *C* and *D*). Thus, Alx does not seem to play a role comparable to MntP in manganese export activity, at least under these growth conditions. Although initially surprising, these data are consistent with the inference from the phyletic pattern that Alx and MntP have separate functions in cells.

To gain further insight into the cellular function of Alx, we examined cells without *alx*. Expression of *alx* in *E. coli* is induced by high levels of manganese as well as by alkaline pH conditions (31, 37–39). Thus, we tested whether cells lacking *alx* would be less resistant to high $MnCl_2$ or to high pH conditions. Interestingly, Δ*alx* cells grew similarly to wildtype cells on LB medium with various concentrations of $MnCl_2$ up to 4 mM and with varying pH values ranging from 7.0 to 8.5. Thus, Δ*alx* cells did not display a sensitivity to high $MnCl_2$, high pH, or both high $MnCl_2$ and high pH together. Moreover, Δ*alx* Δ*mntP* double deletion cells did not exhibit an enhanced sensitivity to $MnCl_2$ relative to Δ*mntP* cells. (Fig. S1).

To examine whether Alx expression could alter intracellular manganese levels, despite its not rescuing the manganese sensitivity as MntP and MneA did, we carried out ICP-MS analysis from cells grown in LB containing 0.5 mM $MnCl_2$. Surprisingly, the Δ*mntP* strain expressing Alx had a 4-fold higher intracellular concentration of manganese than the Δ*mntP* strain with the empty vector (Table 1). Thus, Alx expression leads to an increase in manganese levels in cells rather than a decrease, showing that it does not mediate manganese export. Rather it might function in an opposite capacity to enable manganese import.

We also examined whether Alx expression affected other metal levels by performing ICP-MS analysis from cells grown in LB medium. Relative to the Δ*mntP* strain with the empty vector, the Δ*mntP* strain expressing Alx had 1.8-fold lower levels of zinc, 1.2-fold lower levels of copper, and 1.1-fold higher levels of nickel (Table 2). Zinc levels were significantly higher than previously observed (34), which could be due to the strain background, the Δ*mntP* mutation, or other factors. These results

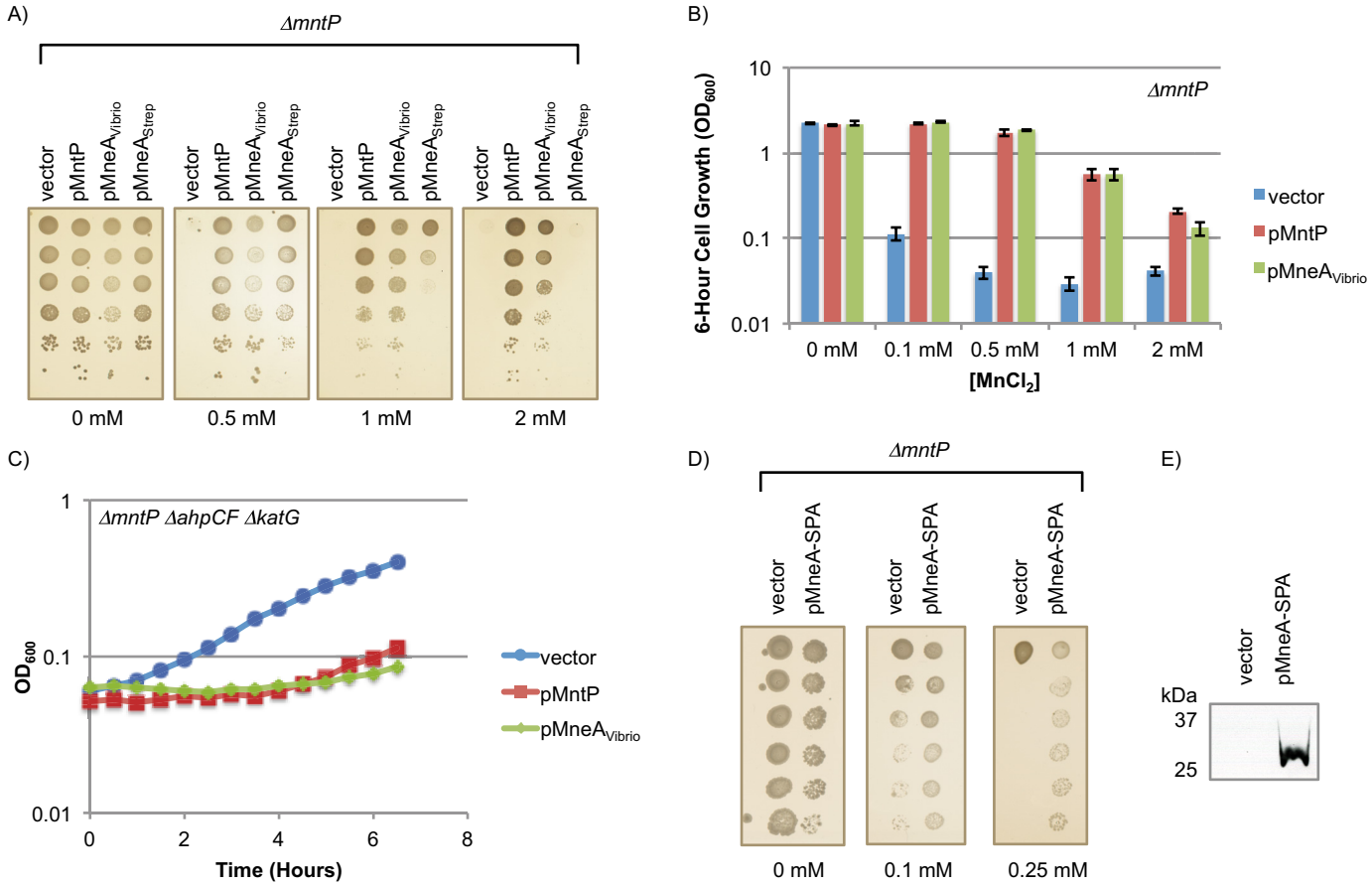

Figure 6. The MneA protein (UPF0016) can provide manganese resistance to Δ*mntP* cells lacking a manganese exporter and confer H_2O_2 sensitivity upon ectopic expression. *A*, the MneA protein complements the manganese sensitivity growth defect of the Δ*mntP* strain. 10-fold serial dilutions of mid-exponential–phase cultures of Δ*mntP* cells (MS047) bearing the pBAD24 empty vector, pBAD24-MntP (pLW132), or pBAD24-MneA cloned from *V. fischeri* (pJS4B) or *Streptomyces* sp. SirexAA-E (pJS1B) were spotted onto LB plates containing 0.2% arabinose, 150 μg/ml ampicillin, and the indicated amounts of $MnCl_2$. *B*, mid-exponential–phase cultures of the strains from *A* were diluted back into LB medium containing 0.2% arabinose, 150 μg/ml ampicillin, and the indicated amounts of $MnCl_2$, and cell growth was monitored after 6 h. *C*, cells ectopically producing MneA under conditions of oxidative stress show a pronounced growth defect similar to those producing MntP. Exponential-phase cultures of Δ*mntP* Δ*ahpCF* Δ*katG* cells (RDZ5) bearing the pBAD24 empty vector, pBAD24-MntP (pLW132), or pBAD24-MneA cloned from *V. fischeri* (pJS4B) were grown in M9 minimal medium with 0.2% arabinose and 150 μg/ml ampicillin. *D*, 10-fold serial dilutions of mid-exponential–phase cultures of Δ*mntP* cells (MS047) bearing the pBAD24 empty vector or pBAD24-MneA-SPA (pKS10) were spotted onto LB plates containing 0.2% arabinose, 150 μg/ml ampicillin, and the indicated amounts of $MnCl_2$. *E*, Western blot analysis of MneA-SPA levels produced from Δ*mntP* cells (MS047) shown in *D*. For *B*, the *error bars* indicate the standard deviations from three replicates of one experiment. For all panels, the data are representative of at least three independent experiments.

Table 1

Intracellular manganese levels in Δ*mntP* cells with the indicated plasmids

Mid-exponential–phase cultures of Δ*mntP* cells (MS047) bearing the pBAD24 empty vector, pBAD24-MneA (pJS4B), or pBAD24-Alx (pJS2B) were diluted into LB containing 0.2% arabinose, 150 μg/ml ampicillin, and 0.5 mM $MnCl_2$ and grown for 2.5 h. Cells were harvested, washed, dried, and used to measure metal levels via ICP-MS. Intracellular metal concentrations were calculated by normalizing metal amounts by total protein levels to correct for mean cell volume. Data are the average of two trials with the indicated range.

Plasmid	Manganese
	μM
Empty vector	92 ± 8
pMneA	34 ± 6
pAlx	364 ± 31

Table 2

Intracellular metal levels in Δ*mntP* cells with the indicated plasmids

Mid-exponential–phase cultures of Δ*mntP* cells (MS047) bearing the pBAD24 empty vector, pBAD24-MneA (pJS4B), or pBAD24-Alx (pJS2B) were diluted into LB containing 0.2% arabinose, and 150 μg/ml ampicillin and grown for 2.5 h. Cells were harvested, washed, dried, and used to measure metal levels via ICP-MS. Intracellular metal concentrations were calculated by normalizing metal amounts by total protein levels to correct for mean cell volume. Data are the average of two trials with the indicated range.

Plasmid	Zinc	Copper	Nickel
	μM	μM	μM
Empty vector	1715 ± 688	35.7 ± 1.1	15.0 ± 1.3
pMneA	1163 ± 649	27.4 ± 11.9	12.9 ± 9.6
pAlx	964 ± 44	29.4 ± 2.2	16.1 ± 3.4

suggest that although Alx may slightly perturb zinc levels, its primary effect is on manganese homeostasis.

When we examined the ability of the Alx protein to inhibit growth in the ROS-sensitized strain background (Δ*ahpCF* Δ*katG*) in M9 minimal medium, we observed that expression of Alx did prevent growth, similar to the exporters MntP and MneA (Fig. 8*E*). Also, like MntP and MneA, supplemental manganese provided in the media could not rescue the growth defect (Fig. S1). This may suggest that Alx affects manganese levels differently under the growth conditions used in this assay (M9 minimal *versus* LB medium used in the manganese sensitivity assay) or that induction of Alx results in a different physiological state from that which allows manganese to combat reactive oxygen species stress. Taken

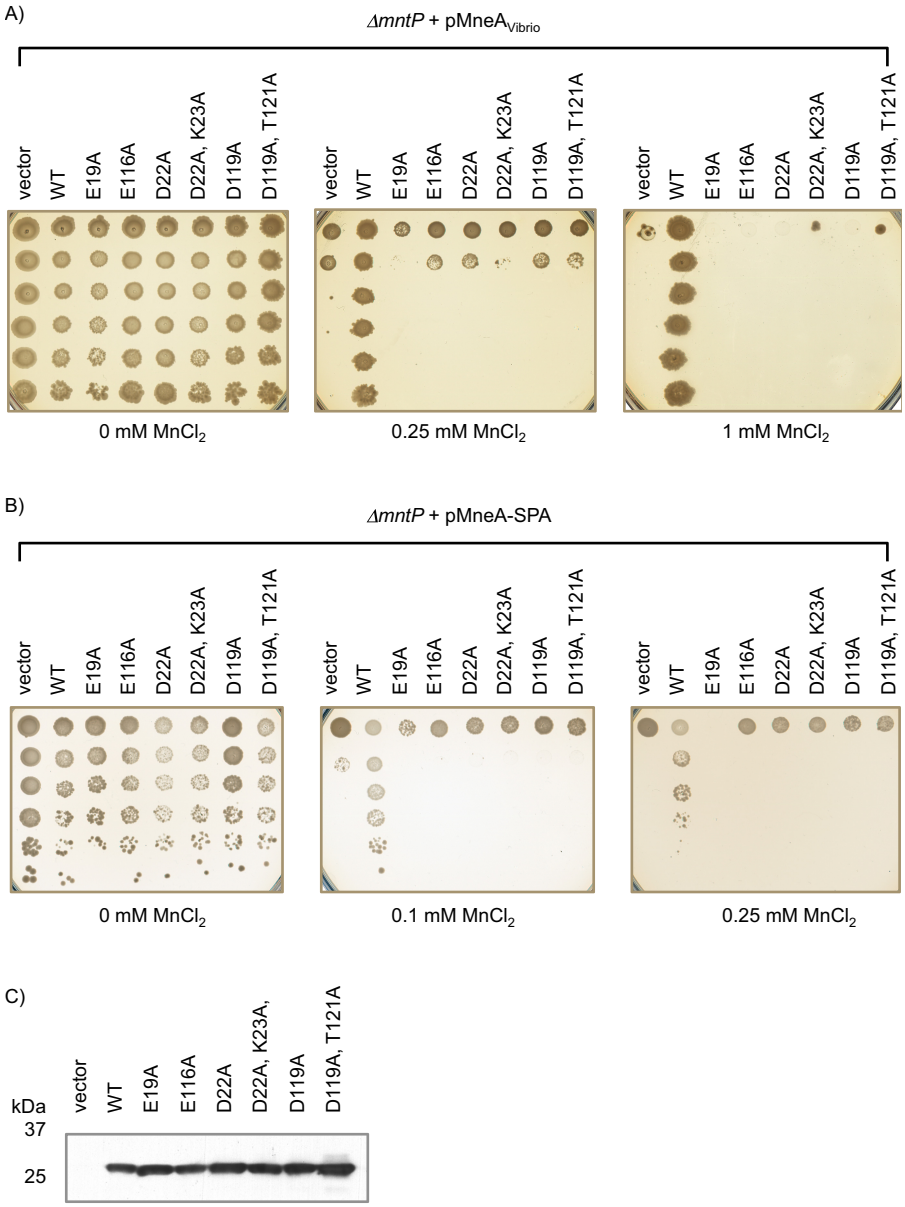

Figure 7. Mutations in conserved charged or polar amino acids impair MneA activity and lead to manganese sensitivity. *A*, epitope-tagged MneA mutants display manganese resistance similar to that of the untagged constructs. 10-fold serial dilutions of mid-exponential–phase cultures of Δ*mntP* cells (MS047) bearing the pBAD24 empty vector, pBAD24-MneA from *V. fischeri* (pJS4B), or pBAD24-MneA from *V. fischeri* with the specified amino acid mutations were spotted onto LB plates containing 0.2% arabinose, 150 μg/ml ampicillin, and the indicated amounts of $MnCl_2$. The mutant pBAD24-MneA plasmids were: pEM9 (E19A), pEM11 (E116A), pEM16 (D22A), pEM24 (D22A,K23A), pEM28 (D119A), and pEM43 (D119A,T121A). *B*, 10-fold serial dilutions of mid-exponential–phase cultures of Δ*mntP* cells (MS047) bearing the pBAD24 empty vector, pBAD24-MneA-SPA (pKS10), or pBAD24-MneA with the specified amino acid mutations were spotted onto LB plates containing 0.2% arabinose, 150 μg/ml ampicillin, and the indicated amounts of $MnCl_2$. The mutant pBAD24-MneA-SPA plasmids used were: pLW179 (E19A), pLW180 (E116A), pLW181 (D22A), pLW182 (D22A,K23A), pLW183 (D119A), and pLW184 (D119A,T121A). *C*, Western blot analysis of MneA-SPA protein levels produced from Δ*mntP* cells (MS047) shown in *A* bearing the pBAD24 empty vector, pBAD24-MneA-SPA (pKS10), or pBAD24-MneA-SPA with the amino acid mutations specified in *B*. For all panels, the data are representative of at least three independent experiments.

together, these results suggest that Alx increases manganese levels and contributes to cell growth during conditions when the amount of manganese is important but that its mechanism of action is not primarily through manganese export, as for MntP and MneA.

Discussion

In this study, we investigated the structure–function relationship of the MntP manganese exporter with other known or predicted export proteins. A combination of computational and experimental approaches was used to define critical amino acids for MntP activity. These assays were also used to characterize other predicted manganese export proteins. We confirmed one protein as a manganese exporter (MneA) with an orthologous function to MntP and, conversely, showed that a related candidate protein (Alx) does not export manganese under similar conditions.

Identification of acidic residues critical for MntP function

First, we identified important residues for manganese efflux by the MntP exporter, summarized in a model derived from the computational analyses (Figs. 2*A* and 9*A*). As observed previ-

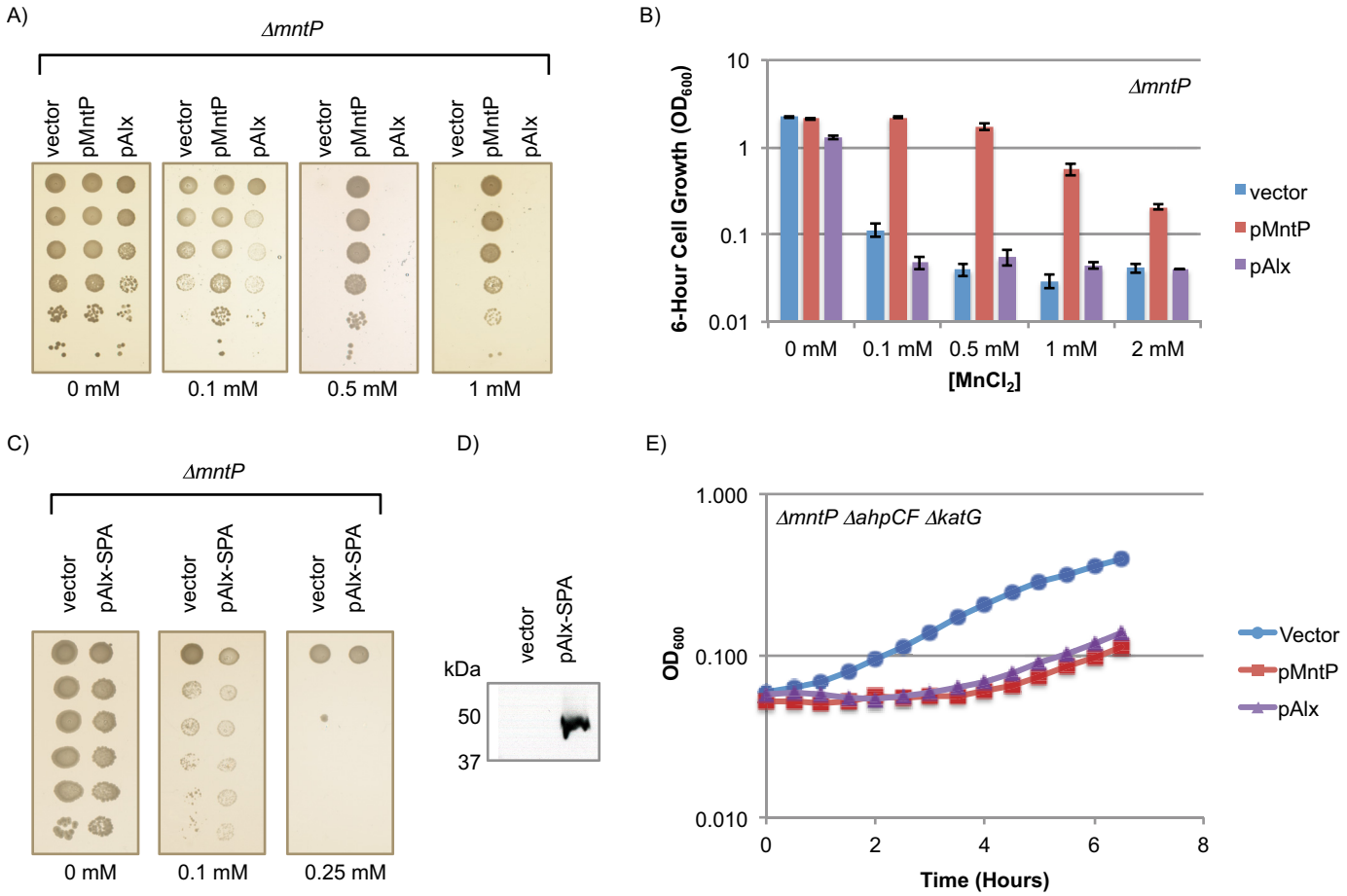

Figure 8. The Alx protein (TerC) cannot provide manganese resistance to the Δ*mntP* cells lacking a manganese exporter but does confer H_2O_2 sensitivity upon ectopic expression. *A*, the Alx protein cannot complement the manganese sensitivity growth defect of the Δ*mntP* strain. 10-fold serial dilutions of mid-exponential–phase cultures of Δ*mntP* cells (MS047) bearing the pBAD24 empty vector, pBAD24-MntP (pLW132), or pBAD24-Alx (pJS2B) were spotted onto LB plates containing 0.2% arabinose, 150 μg/ml ampicillin, and the indicated amounts of $MnCl_2$. The pBAD24 and pBAD24-MntP control data are also presented in Fig. 1*A*. *B*, mid-exponential–phase cultures of the strains from *A* were diluted back into LB medium containing 0.2% arabinose, 150 μg/ml ampicillin, and the indicated amounts of $MnCl_2$, and cell growth was monitored after 6 h. *C*, 10-fold serial dilutions of mid-exponential–phase cultures of Δ*mntP* cells (MS047) bearing the pBAD24 empty vector or pBAD24-Alx-SPA (pKS11) were spotted onto LB plates containing 0.2% arabinose, 150 μg/ml ampicillin, and the indicated amounts of $MnCl_2$. *D*, Western blot analysis of Alx-SPA levels produced from Δ*mntP* cells (MS047) shown in *C*. *E*, cells ectopically producing Alx under conditions of oxidative stress show a pronounced growth defect similar to those producing MntP. Exponential-phase cultures of Δ*mntP* Δ*ahpCF* Δ*katG* cells (RDZ5) bearing the pBAD24 empty vector, pBAD24-MntP (pLW132), or pBAD24-Alx (pJS2B) were grown in M9 minimal medium with 0.2% arabinose and 150 μg/ml ampicillin. For *B*, the *error bars* indicate the standard deviations from three replicates of one experiment. For all panels, the data are representative of at least three independent experiments.

ously, the Asp-16 and Asp-118 amino acids of MntP are among the most conserved in the entire protein (21). The striking conservation of negatively charged amino acids in the center of transmembrane regions led to the prediction that these amino acids would be required for function, and indeed mutation of Asp-16 or Asp-118 completely abolishes MntP activity. These amino acids likely create a negatively charged conduit for manganese in the membrane to export the ion from cells. Three other negatively charged amino acids (Glu-35, Glu-47, and Glu-167) are also important for MntP activity. In some MntP orthologs, these residues are polar, suggesting that they could potentially facilitate the formation of an aqueous binding pocket for manganese. Two of these residues are located in the predicted cytoplasmic loops, which could help capture manganese from the cytoplasm.

Although His residues are known to coordinate manganese in other proteins, the two His amino acids we examined did not contribute to MntP function. We also investigated the role of the highly negatively charged linker between the two trihelical ancestral domains, which we initially hypothesized might serve as a cytoplasmic capture site for manganese. However, this region is poorly conserved in sequence and length when compared across MntP homologs from diverse bacteria. Consistent with this lack of conservation, mutations in this region did not affect MntP activity.

Characterization of the MneA manganese exporter

Using the genomic linkage to the known Mn-responsive *yybP-ykoY* riboswitch regulatory element, we characterized a manganese exporter in the UPF0016 family of proteins. Interestingly, eukaryotic members of the UPF0016 have been recently implicated in human disease. The human representative of this family, TMEM165, is disrupted in the autosomal recessive congenital disorder of glycosylation type 2K, which often manifests as mental and growth retardation (40). The deletion of the yeast ortholog Gdt1 results in sensitivity to high

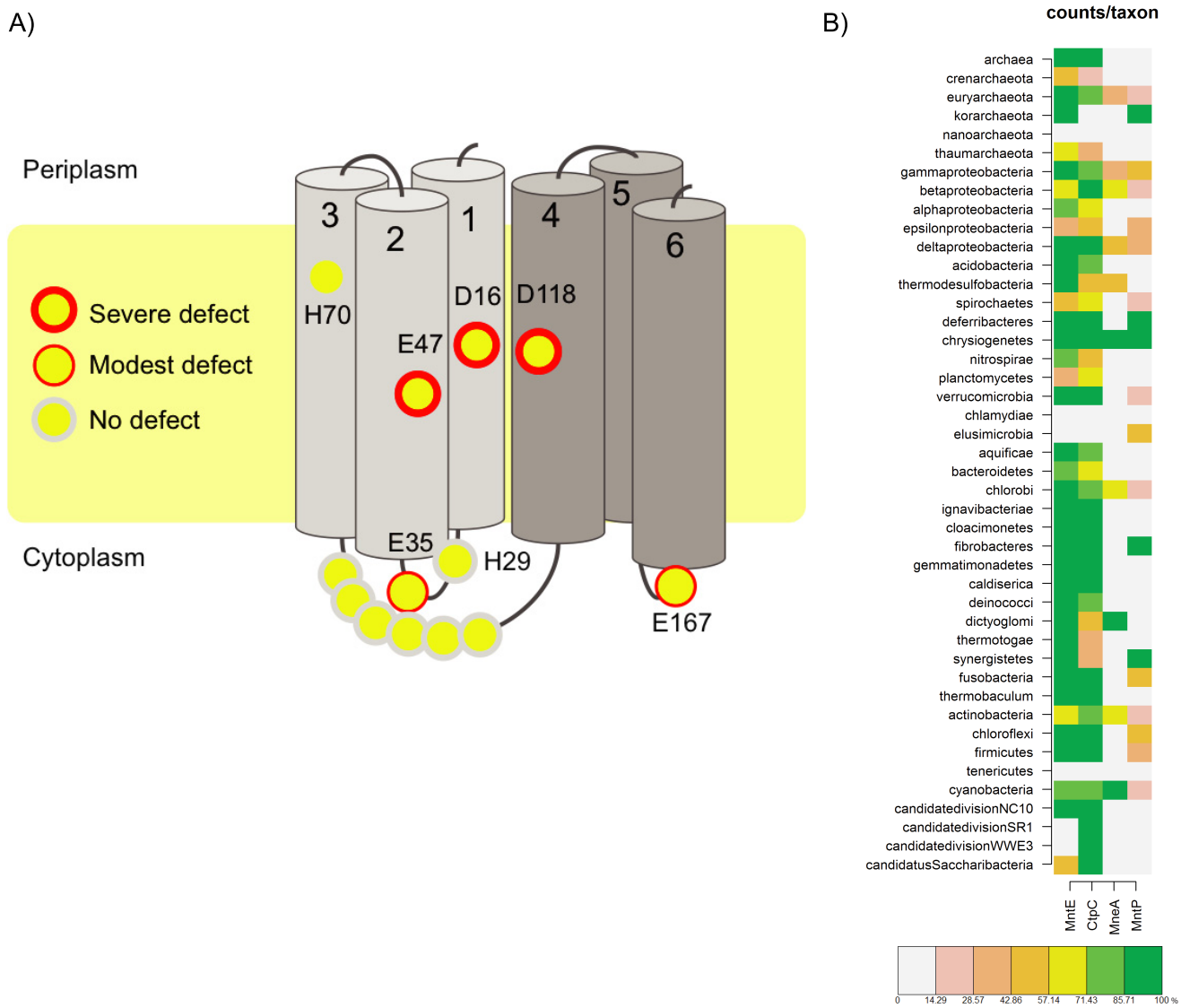

Figure 9. Presence of MntP, MneA, CtpC, and MntE in various clades shows mutual exclusivity of MntP and MneA. *A*, summary of MntP mutants mapped onto the predicted topology of MntP from computational analyses. The first trihelical unit is shown in *light gray* and the second in *dark gray*. *B*, the presence of MntP, MneA, CtpC, and MntE in various clades is shown from high to low prevalence. CtpC and MntE are found throughout prokaryotes, whereas MntP and MneA are more restricted in their distribution and are typically mutually exclusive. The percentage of appearance across prokaryotes is indicated by the color scheme (*dark green* > *green* > *yellow* > *gold* > *pink*).

concentrations of Ca^{2+}, which is complemented by over-expression of human TMEM165 (41). However, the actual ion transported by them has not been conclusively demonstrated (40, 41). The *Vibrio mneA* gene did not confer resistance to calcium in *E. coli* (data not shown). Moreover, another eukaryotic member of the family PAM71 from *Arabidopsis thaliana* has been shown recently to play a role in the sequestration of manganese in chloroplasts (42). We also note that while this work was in progress, an independent study has demonstrated that the UPF0016 family protein from *Vibrio cholerae* functions as a manganese exporter (36). In light of these results and our current findings, it is possible that manganese transport is the primary role of this entire family.

Both MneA and MntP belong to a specific clade of the LysE superfamily along with other families of transporters implicated in heavy metal resistance. This clade is characterized by the striking conservation of an acidic residue within the first TM helix and has emerged from an ancestral 3TM domain. The duplication of this domain is widely observed across the clade, although the MneA family features some versions with a single copy. This implies that in the 6TM versions the two 3TM dyads would necessarily be oriented in the opposite direction. It is possible that this orientation places the conserved acidic residues from the two copies of the 3TM domain in an appropriate configuration to allow metal export. The presence of multiple heavy metal resistance families within this clade of transporters, which have diversified primarily in bacteria, suggests that they all radiated as part of the emergence of resistance to multiple heavy metals and metalloids.

Overall in prokaryotes the function of manganese transport has been roughly evenly split between the two families of transporters that share an ancient common ancestry: MntP is found in 28.7% of organisms from a diverse set selected from across the prokaryotic superkingdoms, and 24% of them (mutually

exclusively) possess MneA (Fig. 9*B*). However, within major prokaryotic lineages there are significant differences in their distributions. For instance, 35% of the proteobacteria possess MntP and ~29% possess MneA, whereas in firmicutes, MntP is the clearly dominant transporter, with 42% of the organisms possessing it in contrast to just ~7% with MneA. Strikingly, in the other major Gram-positive clade, the actinobacteria, this distribution is inverted, with 58% possessing MneA and just 15% possessing MntP. This points to a clade-specific preference for one family of exporter over the other. Although MntP and MneA show a strong tendency for exclusion with respect to each other, neither of them presents such an exclusionary relationship with CtpC or MntE. Around 75 and 76% of the prokaryotes in our survey, respectively, coded for a CtpC-related P-type ATPase and MntE-like CDF transporter in their genomes, including two recently characterized *Bacillus subtilis* CDF-family manganese exporters (43). Strikingly, neither of these transporters ever showed a linkage to the *yybP-ykoY* riboswitch. These observations strongly suggest that the CtpC and MntE exporters perform distinct roles in metal export, perhaps in a more generic capacity than MntP or MneA.

Characterization of the Alx protein

Of the families belonging to the higher-order clade of the LysE superfamily identified here, certain members of the TerC family typified by the eponymous protein have been implicated previously in export of the heavy metalloid tellurium (44). However, the versions of this family prototyped by Alx have remained enigmatic. A large fraction of the Alx-like TerC family genes are associated with the manganese-sensing *yybP-ykoY* riboswitch. In bacteria where *terC* is not associated with the riboswitch, the Alx-like TerC domains are fused to a CorC domain, which we predict to be a metal-binding domain, based on sequence and structure analysis. In *Salmonella typhimurium*, a protein with the CorC domain has been implicated in resistance and efflux of cobalt and magnesium (45). Together, these observations predict a role for the TerC family in coping with metal toxicity.

Here, we have provided the first phenotypic and biochemical evidence examining the role of the Alx protein in manganese homeostasis. Although *alx* levels are induced by manganese, expression of the Alx protein could not restore growth to the Δ*mntP* strain in the presence of $MnCl_2$ in LB medium. Nevertheless, like MntP and MneA, which caused decreased intracellular manganese levels, Alx expression led to a growth defect in a ROS-sensitized strain background that requires high levels of manganese for growth. However, in contrast to MntP or MneA, expression of Alx led to increased levels of intracellular manganese. This is paradoxical because higher intracellular manganese levels are required for a robust ROS response, and Alx increased manganese levels, yet its overproduction led to ROS toxicity. Taken together, these observations suggest that although Alx does not directly export manganese, it might play a distinct, rather unexpected role in the response to manganese toxicity. One possibility is that its metal transport activity has a specialized sensory function. In this context, it is notable that all of the known bacterial sensors for manganese, including riboswitches and the metal-binding motifs of the Fur family of transcription factors, are located intracellularly. This would imply that to effectively and preemptively sense a potential threat from rising external manganese concentrations, the metal needs to be first imported to prime the intracellular sensors to up-regulate genes involved in the manganese response. Our observations suggest that Alx could play such a role. Another not mutually exclusive possibility is that Alx may increase intracellular manganese levels to maintain preparedness for the ROS response in specific conditions, such as high alkalinity. It is clear that cells carefully monitor the level of intracellular manganese and have many layers of regulation for proteins involved manganese homeostasis (*e.g.* the MntR-mediated transcriptional and riboswitch-mediated translational control of MntP expression in *E. coli*). In this context, Alx may provide yet another mechanism to control manganese levels.

Experimental procedures

Strains and plasmids

The strains, plasmids, and oligonucleotide primers used in this study are listed in Tables S1, S2, and S3. Chromosomal deletion strains were generated using pKD4 via mini-λ Red recombineering (46, 47). Deletion constructs were moved into other genetic backgrounds by P1 phage transduction. When needed, the kanamycin resistance marker was removed via the Flp recognition target (FRT) sites with pCP20 (48).

Plasmids were generated by amplifying the open reading frames for *mntP*, *mneA*, and *alx* by PCR from bacterial chromosomal DNA. The products were digested with EcoRI and HindIII and ligated into similarly digested pBAD24 (49). Site-directed mutations were produced in the resulting plasmids via PCR with primers containing mutations in the center of the sequence using Pfu Turbo DNA polymerase as described previously (15). Epitope-tagged constructs used the SPA tag from pJL148 (50). A KpnI site was added just before the stop codon of MntP and the SPA epitope tag preceded by a linker containing the PreScission protease site (LEVLSQGP) was inserted on the C terminus of MntP. Epitope-tagged MneA and Alx were created using the HiFi DNA assembly cloning kit (New England Biolabs). The PreScission linker and SPA epitope tag were inserted on the C termini of MneA and Alx. The resulting MntP-SPA and MneA-SPA constructs were less active than the untagged MntP or MneA but could still partially rescue the manganese sensitivity defect of the Δ*mntP* strain.

E. coli cultures were routinely grown in LB or M9 minimal medium (Difco) with 150 μg/ml ampicillin, 30 μg/ml kanamycin, 0.2% D-glucose, or 0.2% L-arabinose as needed. LB medium was buffered with 0.1 mM Bistris propane to the indicated pH values.

Manganese sensitivity assays

The Δ*mntP* strain (MS047) bearing the pBAD24 empty vector or indicated plasmids was grown overnight at 37 °C in LB–ampicillin, diluted 1:2000 into LB–ampicillin, and grown for 2.5 h to an A_{600} of ~0.25. Arabinose was added to induce gene expression, and cells were grown for 30 min. Several assays were then used to demonstrate the reproducibility and significance of the growth defects. For the semiquantitative plate-based spot assays, aliquots of 3 μl of 10-fold serial dilutions

were spotted onto LB plates with ampicillin and arabinose containing the indicated concentrations of $MnCl_2$. Each spot represents the effect of 1 order of magnitude. For the plate-based colony-forming unit assay, 10-fold serial dilutions of three independent cultures were made, and 100 μl of the appropriate dilution for each culture was plated on duplicate LB plates with ampicillin and arabinose containing the indicated concentrations of $MnCl_2$. For the liquid growth assays, after growth of three independent cultures in LB–ampicillin–arabinose for 30 min, the strains were diluted back to an A_{600} of ~0.003 in LB–ampicillin with arabinose, and the A_{600} was measured every hour. Full growth curves were performed (Figs. S2–S5) as described in the supporting Experimental procedures. For clarity, a 6-h time point was chosen to present (Figs. 1*C*, 3*B*, 6*B*, and 8*B*).

H_2O_2 sensitivity assay

The Δ*mntP* Δ*ahpCF* Δ*katG* strain (RDZ5) bearing the pBAD24 empty vector or indicated plasmids was initially grown overnight at 37 °C in M9 – glucose–ampicillin containing 10 μM $MnCl_2$ and 10 mM pyruvate to provide protection against the high-internal cellular levels of H_2O_2. Cells were diluted to an A_{600} of ~0.002 in 20 ml of the same medium and grown overnight at 30 °C to obtain log-phase cultures. Cells were washed twice in M9 medium to remove glucose and resuspended in 20 ml of M9 –arabinose–ampicillin lacking $MnCl_2$ or pyruvate. If needed, cultures were normalized to an A_{600} of ~0.1. Growth was followed by monitoring A_{600} at 37 °C.

Western blot analysis

For Western blot analysis, an aliquot of cells grown for the manganese sensitivity assay was collected by centrifugation immediately before cells were spotted onto plates. Cells were lysed by resuspension in 1× SDS loading buffer with 100 mM dithiothreitol by heating at 37 °C for 30 min. Incubation at this temperature greatly decreased MntP aggregation and increased the amount of MntP protein that migrated into the gel for detection. The whole-cell lysate corresponding to ~0.03 A_{600} units of cells was separated on 4–20% Tris-glycine gels (Bio-Rad) (Fig. 4) or 12% Tris-glycine gels (Figs. 6*E* and 8*D*) and transferred to nitrocellulose membranes (Bio-Rad). To detect Alx-SPA, ~0.005 A_{600} units of cells were used (Fig. 8*D*). Membranes were blocked with 2% milk in Tris-buffered saline with Tween-20 (TBS-T) and probed with 1:1000 anti-FLAG M2-AP antibody (Sigma-Aldrich) in 2% milk–TBS-T. Signals were visualized using LumiPhos WB (Pierce).

ICP-MS for measurement of total cell-associated metal

The total amounts of cell-associated metals were quantified from 5-ml cultures that had been grown in LB–ampicillin with arabinose and, if indicated, 0.5 mM $MnCl_2$ for 2.5 h after dilution to ~0.01 A_{600}. Cells were centrifuged, washed once with 10 mM HEPES, pH 7.5, containing 2 mM EDTA, washed twice with 10 mM HEPES, and dried for 1 h using a centrifuge evaporator. The dried cells were solubilized in 400 μl of 30% (v/v) HNO_3 and lysed by incubating them at 95 °C for 10 min of shaking at 500 rpm. ICP-MS samples were prepared by diluting 300 μl of lysed cells into 2.7 ml of 2.5% (v/v) HNO_3 and run on an ELAN DRC II instrument (PerkinElmer). Metal concentrations are presented as intracellular levels after correction for mean cell volume determined from total protein content. Concentrations were calculated from the standard curve using 1–30 ppb metal stock solutions and normalized to total protein determined using a DC™ protein assay (Bio-Rad) as described (15, 33). The data presented are an average of two trials.

Methods for computational analysis

A database of protein sequences from 2726 complete prokaryotic genomes (National Center for Biotechnology Information, National Institutes of Health, Bethesda, MD) was searched iteratively using the PSI-BLAST program with *E. coli* MntP and the *V. fischeri* MneA proteins as the query and with a position-specific scoring matrix (PSSM) inclusion expectation (*E*) value threshold of 0.01 (51). The searches were iterated until convergence (52, 53). Transmembrane regions were predicted in individual proteins using the TMHMM2.0 and Phobius programs with default parameters (54, 55). Multiple alignments were constructed using the Kalign program followed by manual correction based on PSI-BLAST results (56, 57). All large-scale sequence analysis procedures were carried out using the TASS package developed by our group.[6] Protein secondary structure was predicted using a multiple alignment as the input for the JPRED program (58). Similarity-based clustering of proteins was carried out using the BLASTCLUST program.

Author contributions—L. S. W. designed the study, performed and analyzed the experiments, and wrote the paper. L. A. and V. A. performed the computational analyses, prepared Figs. 2 and 9*B*, and wrote the paper. R. Z., E. M., J. S., K. S., and B. U. generated vectors for the expression of mutant proteins and analyzed the mutant phenotypes in bacteria. All authors reviewed the results and approved the final version of the manuscript.

Acknowledgments—We thank G. Storz and M. Hemm for helpful discussions; C. Bianchetti, C. Wimpee, and M. Dambach for the kind gift of bacterial strains; and Julia E. Martin and Jiefei Wang from David P. Giedroc's laboratory for the ICP-MS analysis.

References

1. Waldron, K. J., and Robinson, N. J. (2009) How do bacterial cells ensure that metalloproteins get the correct metal? *Nat. Rev. Microbiol.* **7,** 25–35 CrossRef Medline
2. Waldron, K. J., Rutherford, J. C., Ford, D., and Robinson, N. J. (2009) Metalloproteins and metal sensing. *Nature* **460,** 823–830 CrossRef Medline
3. Lisher, J. P., and Giedroc, D. P. (2013) Manganese acquisition and homeostasis at the host-pathogen interface. *Front. Cell. Infect. Microbiol.* **3,** 91 Medline
4. Hood, M. I., and Skaar, E. P. (2012) Nutritional immunity: Transition metals at the pathogen-host interface. *Nat. Rev. Microbiol.* **10,** 525–537 CrossRef Medline
5. Martin, J. E., and Giedroc, D. P. (2016) Functional determinants of metal ion transport and selectivity in paralogous cation diffusion facilitator transporters CzcD and MntE in *Streptococcus pneumoniae*. *J. Bacteriol.* **198,** 1066–1076 CrossRef Medline
6. Imlay, J. A. (2014) The mismetallation of enzymes during oxidative stress. *J. Biol. Chem.* **289,** 28121–28128 CrossRef Medline

[6] V. Anantharaman and L. Aravind, unpublished results.

7. Barras, F., and Fontecave, M. (2011) Cobalt stress in *Escherichia coli* and *Salmonella enterica*: Molecular bases for toxicity and resistance. *Metallomics* **3,** 1130–1134 CrossRef Medline
8. Macomber, L., and Hausinger, R. P. (2011) Mechanisms of nickel toxicity in microorganisms. *Metallomics* **3,** 1153–1162 CrossRef Medline
9. Ma, Z., Jacobsen, F. E., and Giedroc, D. P. (2009) Coordination chemistry of bacterial metal transport and sensing. *Chem. Rev.* **109,** 4644–4681 CrossRef Medline
10. Porcheron, G., Garénaux, A., Proulx, J., Sabri, M., and Dozois, C. M. (2013) Iron, copper, zinc, and manganese transport and regulation in pathogenic enterobacteria: Correlations between strains, site of infection and the relative importance of the different metal transport systems for virulence. *Front. Cell. Infect. Microbiol.* **3,** 90 Medline
11. Sobota, J. M., and Imlay, J. A. (2011) Iron enzyme ribulose-5-phosphate 3-epimerase in *Escherichia coli* is rapidly damaged by hydrogen peroxide but can be protected by manganese. *Proc. Natl. Acad. Sci. U.S.A.* **108,** 5402–5407 CrossRef Medline
12. Anjem, A., and Imlay, J. A. (2012) Mononuclear iron enzymes are primary targets of hydrogen peroxide stress. *J. Biol. Chem.* **287,** 15544–15556 CrossRef Medline
13. Kehres, D. G., and Maguire, M. E. (2003) Emerging themes in manganese transport, biochemistry and pathogenesis in bacteria. *FEMS Microbiol. Rev.* **27,** 263–290 CrossRef Medline
14. Papp-Wallace, K. M., and Maguire, M. E. (2006) Manganese transport and the role of manganese in virulence. *Annu. Rev. Microbiol.* **60,** 187–209 CrossRef Medline
15. Martin, J. E., Waters, L. S., Storz, G., and Imlay, J. A. (2015) The *Escherichia coli* small protein MntS and exporter MntP optimize the intracellular concentration of manganese. *PLoS Genet.* **11,** e1004977 CrossRef Medline
16. Martin, J. E., Lisher, J. P., Winkler, M. E., and Giedroc, D. P. (2017) Perturbation of manganese metabolism disrupts cell division in *Streptococcus pneumoniae*. *Mol. Microbiol.* **104,** 334–348 CrossRef Medline
17. Hohle, T. H., and O'Brian, M. R. (2014) Magnesium-dependent processes are targets of bacterial manganese toxicity. *Mol. Microbiol.* **93,** 736–747 CrossRef Medline
18. Helmann, J. D. (2014) Specificity of metal sensing: Iron and manganese homeostasis in *Bacillus subtilis*. *J. Biol. Chem.* **289,** 28112–28120 CrossRef Medline
19. Rosch, J. W., Gao, G., Ridout, G., Wang, Y. D., and Tuomanen, E. I. (2009) Role of the manganese efflux system *mntE* for signalling and pathogenesis in *Streptococcus pneumoniae*. *Mol. Microbiol.* **72,** 12–25 CrossRef Medline
20. Waters, L. S., Sandoval, M., and Storz, G. (2011) The *Escherichia coli* MntR miniregulon includes genes encoding a small protein and an efflux pump required for manganese homeostasis. *J. Bacteriol.* **193,** 5887–5897 CrossRef Medline
21. Veyrier, F. J., Boneca, I. G., Cellier, M. F., and Taha, M. K. (2011) A novel metal transporter mediating manganese export (MntX) regulates the Mn to Fe intracellular ratio and *Neisseria meningitidis* virulence. *PLoS Pathog.* **7,** e1002261 CrossRef Medline
22. Li, C., Tao, J., Mao, D., and He, C. (2011) A novel manganese efflux system, YebN, is required for virulence by *Xanthomonas oryzae* pv. oryzae. *PLoS ONE* **6,** e21983 CrossRef Medline
23. Aleshin, V. V., Zakataeva, N. P., and Livshits, V. A. (1999) A new family of amino-acid-efflux proteins. *Trends Biochem. Sci.* **24,** 133–135 CrossRef Medline
24. Vrljic, M., Garg, J., Bellmann, A., Wachi, S., Freudl, R., Malecki, M. J., Sahm, H., Kozina, V. J., Eggeling, L., Saier, M. H., Jr., Eggeling, L., and Saier, M. H., Jr. (1999) The LysE superfamily: Topology of the lysine exporter LysE of *Corynebacterium glutamicum*, a paradyme for a novel superfamily of transmembrane solute translocators. *J. Mol. Microbiol. Biotechnol.* **1,** 327–336 Medline
25. Padilla-Benavides, T., Long, J. E., Raimunda, D., Sassetti, C. M., and Argüello, J. M. (2013) A novel P(1B)-type Mn^{2+}-transporting ATPase is required for secreted protein metallation in mycobacteria. *J. Biol. Chem.* **288,** 11334–11347 CrossRef Medline
26. Neyrolles, O., Wolschendorf, F., Mitra, A., and Niederweis, M. (2015) Mycobacteria, metals, and the macrophage. *Immunol. Rev.* **264,** 249–263 CrossRef Medline
27. Yamamoto, K., Ishihama, A., Busby, S. J., and Grainger, D. C. (2011) The *Escherichia coli* K-12 MntR miniregulon includes dps, which encodes the major stationary-phase DNA-binding protein. *J. Bacteriol.* **193,** 1477–1480 CrossRef Medline
28. Turner, A. G., Ong, C. L., Gillen, C. M., Davies, M. R., West, N. P., McEwan, A. G., and Walker, M. J. (2015) Manganese homeostasis in group A *Streptococcus* is critical for resistance to oxidative stress and virulence. *MBio* **6,** e00278–e00315 Medline
29. Sun, H., Xu, G., Zhan, H., Chen, H., Sun, Z., Tian, B., and Hua, Y. (2010) Identification and evaluation of the role of the manganese efflux protein in *Deinococcus radiodurans*. *BMC Microbiol.* **10,** 319 CrossRefCrossRef Medline
30. Cubillas, C., Vinuesa, P., Tabche, M. L., Dávalos, A., Vázquez, A., Hernández-Lucas, I., Romero, D., and García-de los Santos, A. (2014) The cation diffusion facilitator protein EmfA of Rhizobium etli belongs to a novel subfamily of Mn(2+)/Fe(2+) transporters conserved in α-proteobacteria. *Metallomics* **6,** 1808–1815 CrossRef Medline
31. Dambach, M., Sandoval, M., Updegrove, T. B., Anantharaman, V., Aravind, L., Waters, L. S., and Storz, G. (2015) The ubiquitous yybP-ykoY riboswitch is a manganese-responsive regulatory element. *Mol. Cell* **57,** 1099–1109 CrossRef Medline
32. Price, I. R., Gaballa, A., Ding, F., Helmann, J. D., and Ke, A. (2015) Mn(2+)-sensing mechanisms of yybP-ykoY orphan riboswitches. *Mol. Cell* **57,** 1110–1123 CrossRef Medline
33. Anjem, A., Varghese, S., and Imlay, J. A. (2009) Manganese import is a key element of the OxyR response to hydrogen peroxide in *Escherichia coli*. *Mol. Microbiol.* **72,** 844–858 Medline
34. Outten, C. E., and O'Halloran, T. V. (2001) Femtomolar sensitivity of metalloregulatory proteins controlling zinc homeostasis. *Science* **292,** 2488–2492 CrossRef Medline
35. Seaver, L. C., and Imlay, J. A. (2001) Hydrogen peroxide fluxes and compartmentalization inside growing *Escherichia coli*. *J. Bacteriol.* **183,** 7182–7189 CrossRef Medline
36. Fisher, C. R., Wyckoff, E. E., Peng, E. D., and Payne, S. M. (2016) Identification and characterization of a putative manganese export protein in *Vibrio cholerae*. *J. Bacteriol.* **198,** 2810–2817 CrossRef Medline
37. Bingham, R. J., Hall, K. S., and Slonczewski, J. L. (1990) Alkaline induction of a novel gene locus, *alx*, in *Escherichia coli*. *J. Bacteriol.* **172,** 2184–2186 CrossRef Medline
38. Stancik, L. M., Stancik, D. M., Schmidt, B., Barnhart, D. M., Yoncheva, Y. N., and Slonczewski, J. L. (2002) pH-dependent expression of periplasmic proteins and amino acid catabolism in *Escherichia coli*. *J. Bacteriol.* **184,** 4246–4258 CrossRef Medline
39. Nechooshtan, G., Elgrably-Weiss, M., Sheaffer, A., Westhof, E., and Altuvia, S. (2009) A pH-responsive riboregulator. *Genes Dev.* **23,** 2650–2662 CrossRef Medline
40. Foulquier, F., Amyere, M., Jaeken, J., Zeevaert, R., Schollen, E., Race, V., Bammens, R., Morelle, W., Rosnoblet, C., Legrand, D., Demaegd, D., Buist, N., Cheillan, D., Guffon, N., Morsomme, P., *et al.* (2012) TMEM165 deficiency causes a congenital disorder of glycosylation. *Am. J. Hum. Genet.* **91,** 15–26 CrossRef Medline
41. Demaegd, D., Foulquier, F., Colinet, A. S., Gremillon, L., Legrand, D., Mariot, P., Peiter, E., Van Schaftingen, E., Matthijs, G., and Morsomme, P. (2013) Newly characterized Golgi-localized family of proteins is involved in calcium and pH homeostasis in yeast and human cells. *Proc. Natl. Acad. Sci. U.S.A.* **110,** 6859–6864 CrossRef Medline
42. Schneider, A., Steinberger, I., Herdean, A., Gandini, C., Eisenhut, M., Kurz, S., Morper, A., Hoecker, N., Rühle, T., Labs, M., Flügge, U. I., Geimer, S., Schmidt, S. B., Husted, S., Weber, A. P., *et al.* (2016) The evolutionarily conserved protein PHOTOSYNTHESIS-AFFECTED MUTANT71 is required for efficient manganese uptake at the thylakoid membrane in *Arabidopsis*. *Plant Cell* **28,** 892–910 Medline
43. Huang, X., Shin, J. H., Pinochet-Barros, A., Su, T. T., and Helmann, J. D. (2017) *Bacillus subtilis* MntR coordinates the transcriptional regulation of

manganese uptake and efflux systems. *Mol. Microbiol.* **103,** 253–268 CrossRef Medline

44. Anantharaman, V., Iyer, L. M., and Aravind, L. (2012) Ter-dependent stress response systems: Novel pathways related to metal sensing, production of a nucleoside-like metabolite, and DNA-processing. *Mol. Biosyst.* **8,** 3142–3165 CrossRef Medline
45. Gibson, M. M., Bagga, D. A., Miller, C. G., and Maguire, M. E. (1991) Magnesium transport in *Salmonella typhimurium*: The influence of new mutations conferring Co^{2+} resistance on the CorA Mg2+ transport system. *Mol. Microbiol.* **5,** 2753–2762 CrossRef Medline
46. Datsenko, K. A., and Wanner, B. L. (2000) One-step inactivation of chromosomal genes in *Escherichia coli* K-12 using PCR products. *Proc. Natl. Acad. Sci. U.S.A.* **97,** 6640–6645 CrossRef Medline
47. Yu, D., Ellis, H. M., Lee, E. C., Jenkins, N. A., Copeland, N. G., and Court, D. L. (2000) An efficient recombination system for chromosome engineering in *Escherichia coli*. *Proc. Natl. Acad. Sci. U.S.A.* **97,** 5978–5983 CrossRef
48. Cherepanov, P. P., and Wackernagel, W. (1995) Gene disruption in *Escherichia coli*: TcR and KmR cassettes with the option of Flp-catalyzed excision of the antibiotic-resistance determinant. *Gene* **158,** 9–14 CrossRef Medline
49. Guzman, L. M., Belin, D., Carson, M. J., and Beckwith, J. (1995) Tight regulation, modulation, and high-level expression by vectors containing the arabinose PBAD promoter. *J. Bacteriol.* **177,** 4121–4130 CrossRef Medline
50. Zeghouf, M., Li, J., Butland, G., Borkowska, A., Canadien, V., Richards, D., Beattie, B., Emili, A., and Greenblatt, J. F. (2004) Sequential peptide affinity (SPA) system for the identification of mammalian and bacterial protein complexes. *J. Proteome Res.* **3,** 463–468 CrossRef Medline
51. Altschul, S. F., and Koonin, E. V. (1998) Iterated profile searches with PSI-BLAST: A tool for discovery in protein databases. *Trends Biochem. Sci.* **23,** 444–447 CrossRef Medline
52. Altschul, S. F., Madden, T. L., Schäffer, A. A., Zhang, J., Zhang, Z., Miller, W., and Lipman, D. J. (1997) Gapped BLAST and PSI-BLAST: A new generation of protein database search programs. *Nucleic Acids Res.* **25,** 3389–3402 CrossRef Medline
53. Aravind, L., and Koonin, E. V. (1999) Gleaning non-trivial structural, functional and evolutionary information about proteins by iterative database searches. *J. Mol. Biol.* **287,** 1023–1040 CrossRef Medline
54. Käll, L., Krogh, A., and Sonnhammer, E. L. (2004) A combined transmembrane topology and signal peptide prediction method. *J. Mol. Biol.* **338,** 1027–1036 CrossRef Medline
55. Krogh, A., Larsson, B., von Heijne, G., and Sonnhammer, E. L. (2001) Predicting transmembrane protein topology with a hidden Markov model: Application to complete genomes. *J. Mol. Biol.* **305,** 567–580 CrossRef Medline
56. Lassmann, T., Frings, O., and Sonnhammer, E. L. (2009) Kalign2: High-performance multiple alignment of protein and nucleotide sequences allowing external features. *Nucleic Acids Res.* **37,** 858–865 CrossRef Medline
57. Lassmann, T., and Sonnhammer, E. L. (2005) Kalign: An accurate and fast multiple sequence alignment algorithm. *BMC Bioinformatics* **6,** 298 CrossRef Medline
58. Cuff, J. A., and Barton, G. J. (2000) Application of multiple sequence alignment profiles to improve protein secondary structure prediction. *Proteins* **40,** 502–511 CrossRef Medline